Supplementary Figure 1. Polymorphism across the genome in all ten species samples. Polymorphism in 1Mb windows across the genome for all ten species samples. Some samples show long stretches of homozygosity indicative of recent inbreeding; this inbreeding could explain the lack of increased polymorphism on chromosome four in *A. aurea*. Similarly, an extended stretch of homozygosity was seen on chromosome four in an additional sample of *A. pubescens* that was used in the construction of our F2 mapping population (**Supplemental Fig. 5**, sample pub.1).

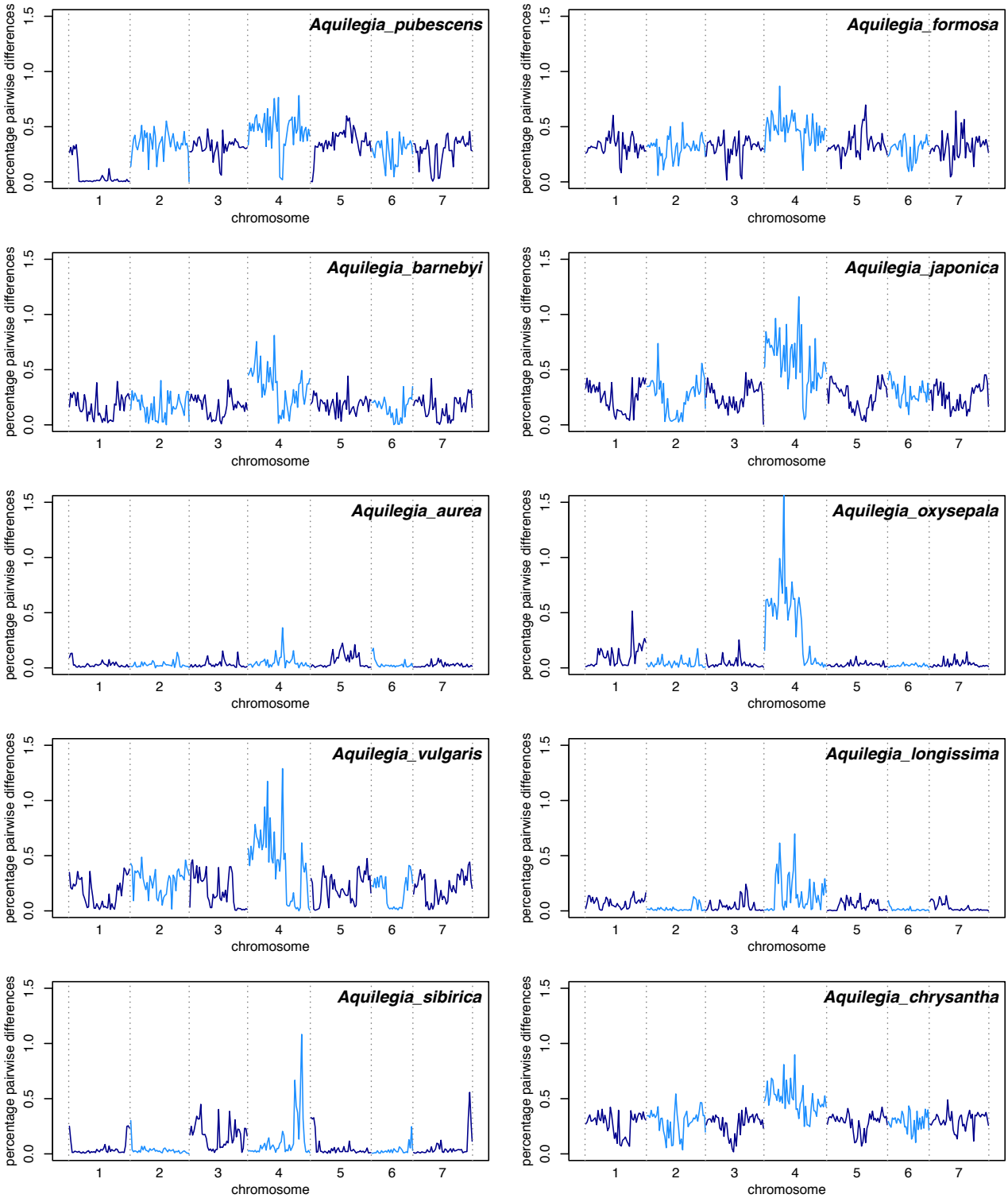

Supplementary Figure 2. Species and chromsome trees of *Aquilegia***.** (a) RAxML tree from concatenated genomic data (b) Neighbor joining tree from concatenated chromosome four data (c) RAxML tree from concatenated chromosome four data. Bootstrap support values are presented for all trees

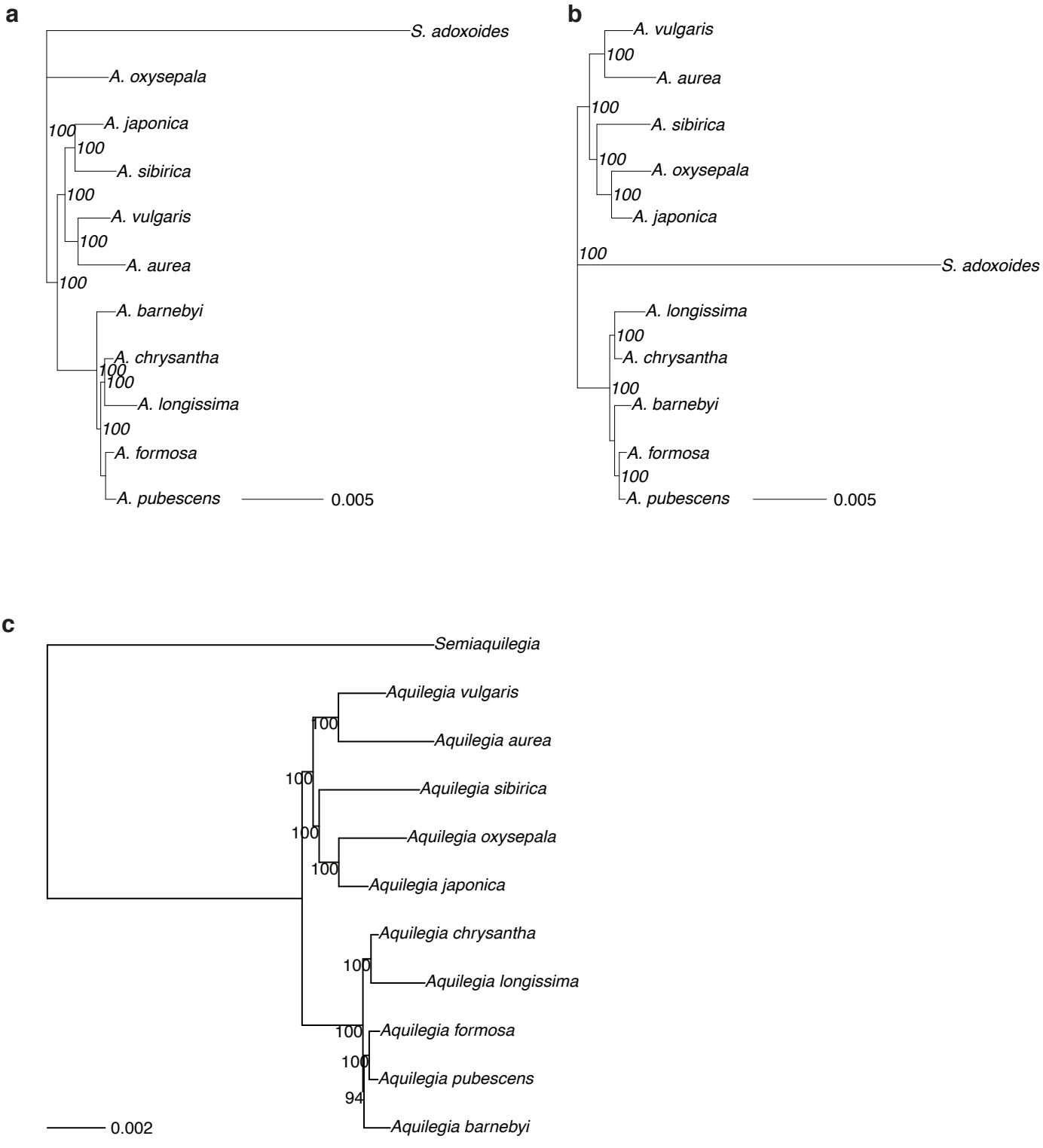

Supplementary Figure 3. Subtree prevalence across chromosomes for the nine significantly-different subtrees.

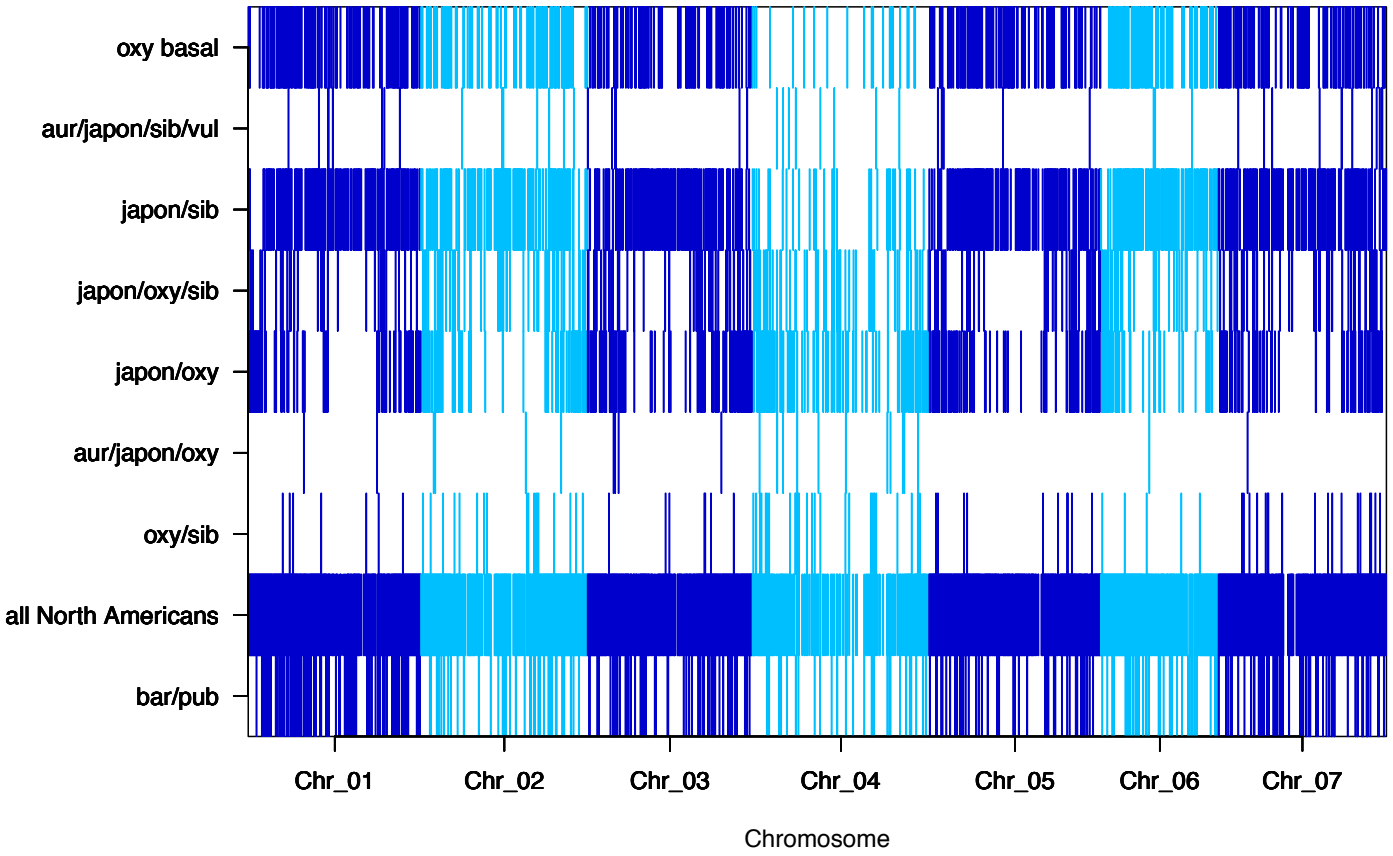

Supplementary Figure 4. Model output for all three gene flow scenarios. Simulated tree topology proportions (left) and D-statistics (right) under models of symmetric (top), asymmetric (middle) and unidirectional gene flow (bottom). Left: Tree topologies are simulated under 100 different combinations of m and N (represented as M on the x-axis) and 10 different combinations of t1 (four values of which are shown in the legend). The difference between each of the 1000 simulated and observed tree topology proportions is estimated using euclidean distance where observed and simulated proportions of sib-fla and fla-oxy topologies specify point 1 and point 2, respectively (sib-fla refers to red tree while fla-oxy refers to blue tree in **Fig. 6a**). Quantified as such, a difference of zero (y-axis) points at the best parameter combination that matches observed allele sharing proportions genomewide. Right: Given the "species" tree (**Fig. 6b**), D-statistics (y-axis) are calculated for different combinations of m (x-axis) and N (legend; top left) which cover the parameter space of interest (**Fig. 6c** and **Supplementary Table 7**). Note that simulations are carried out with t1=1 and only five out of twelve N values are shown in the legend. Filled circles on the y-axis denote observed chromosome-specific D statistic estimates and horizontal black lines denote the range of these values

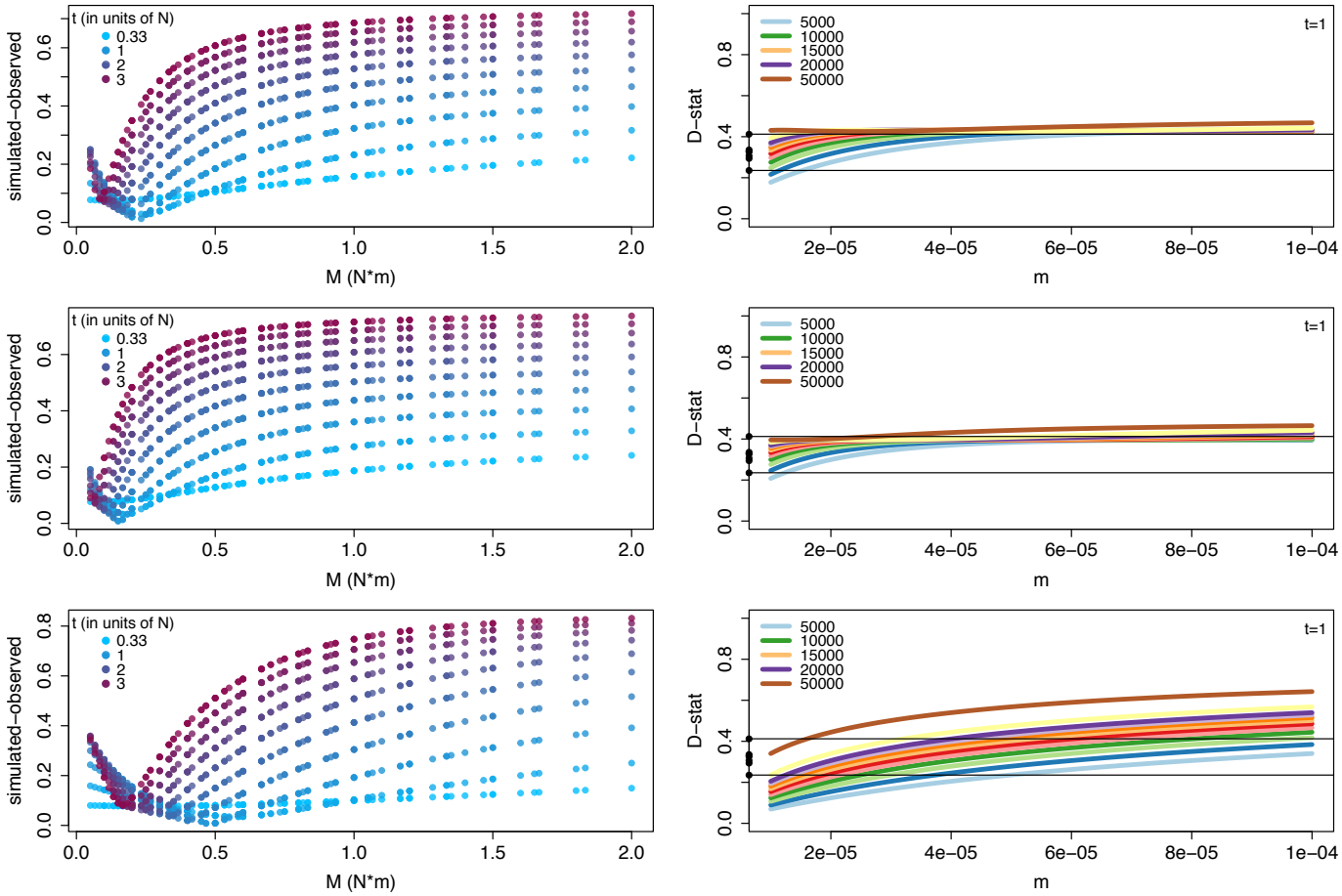

Supplementary Figure 5. Polymorphism and recombination in the *A. formosa* x *A. pubescens* mapping population. (a) Polymorphism by chromosome for mapping population F0s (form.1, form.2, pub.1, and pub.2) and their corresponding F1s (F1.1 and F1.2). Samples form.2 and pub.2 were included in the main data set as *A. formosa* and *A. pubescens*; they are presented again in this figure for clarity. Although polymorphism was not elevated on chromosome four in pub.1, polymorphism was elevated in an F1 constructed using this individual (F1.1). (b) Comparison of physical and genetic maps by chromosome for the cross. (c) Polymorphism across the genome in 1MB windows for the samples in (a). A large inbred region observed on chromosome four in F1.1 suggests that inbreeding is the cause of the non-elevated polymorphism in this sample.

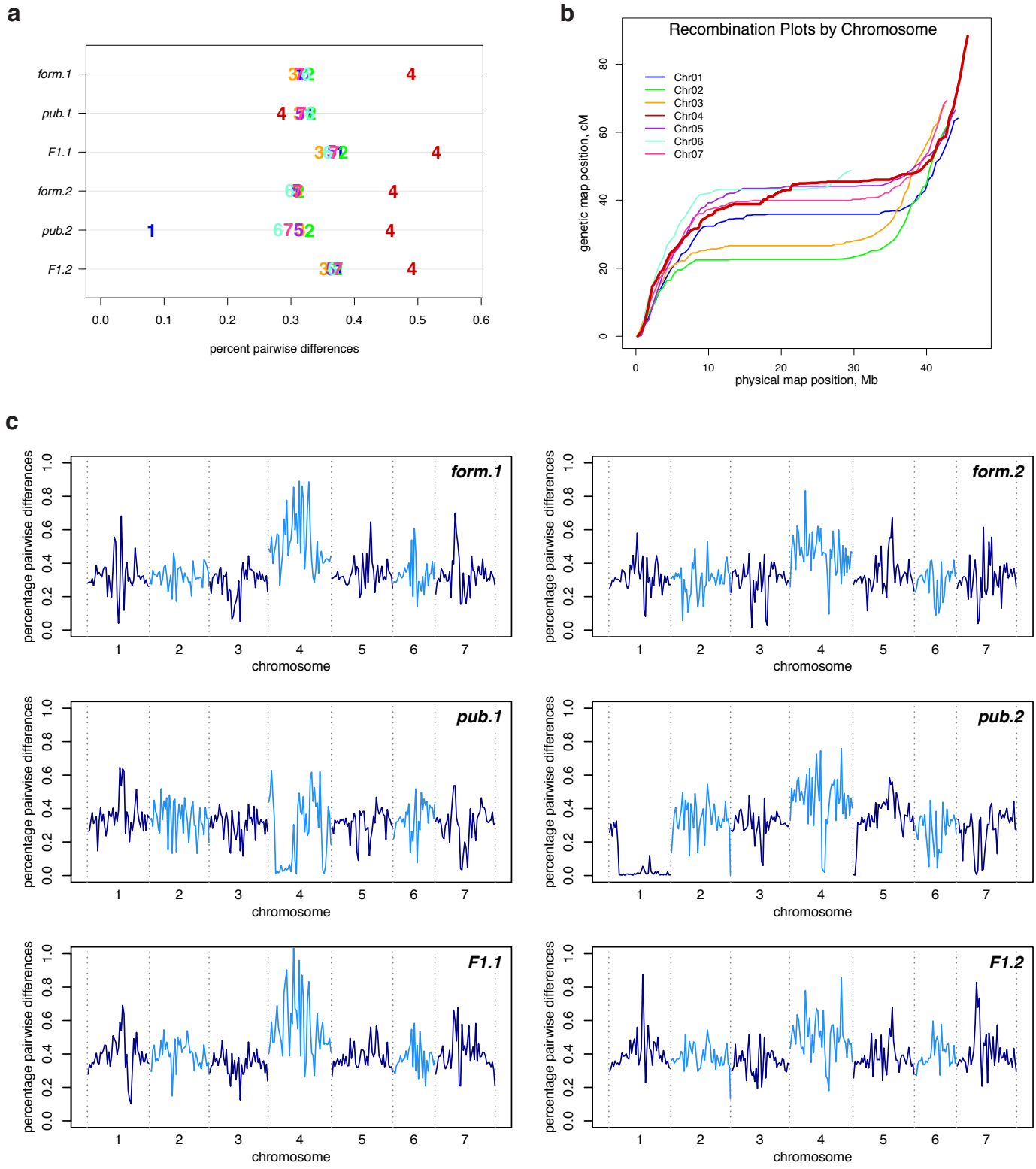

Supplementary Figure 6. Distribution of gene expression values by chromosome.

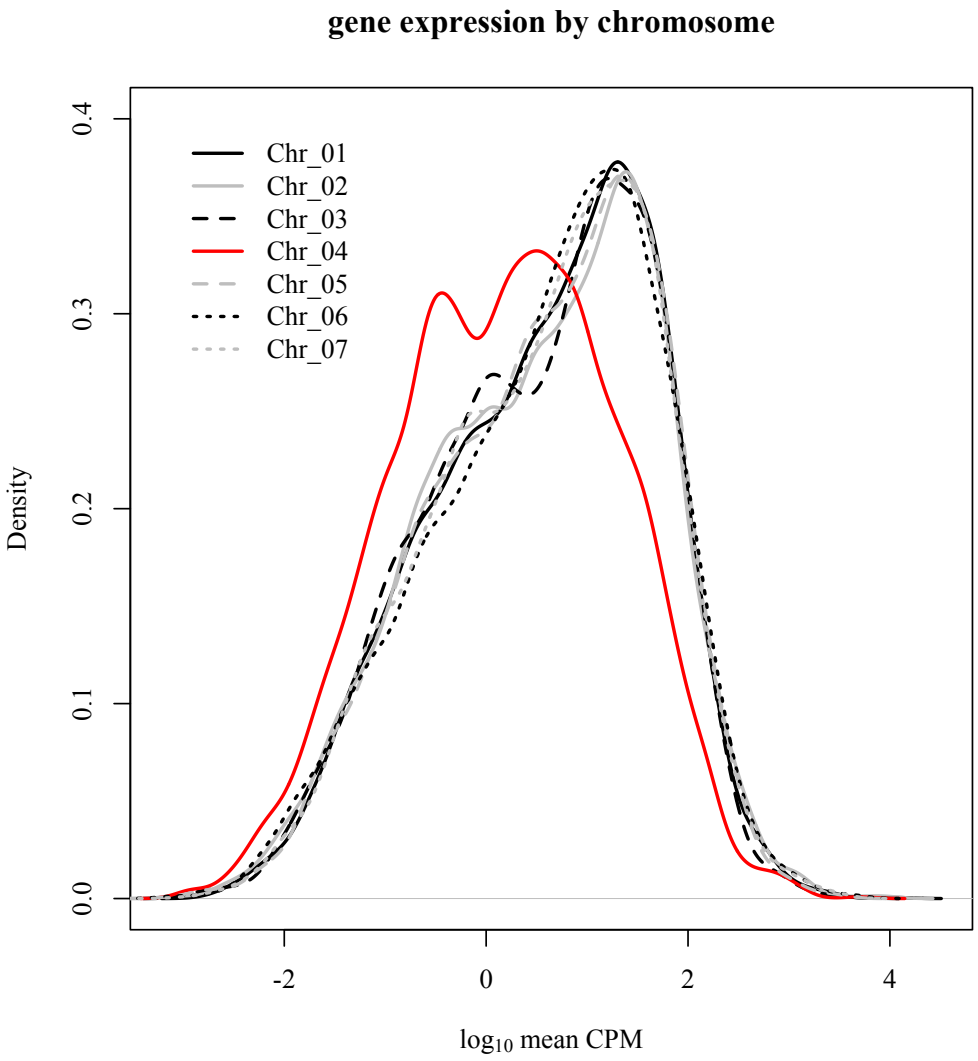

Supplementary Figure 7. Immunodetection of anti-5mC antibody (pink), and FISH of 35S rDNA (green) and oligoCh4 (red) probes on mitotic and pachytene chromosomes in *Semiaquilegia adoxoides*, *Aquilegia vulgaris* and *A. formosa*. Chromosomes were counterstained with DAPI and inverted using Photoshop CS software (Adobe Systems). Scale bars = 10 μm.

Semiaquilegia adoxoides

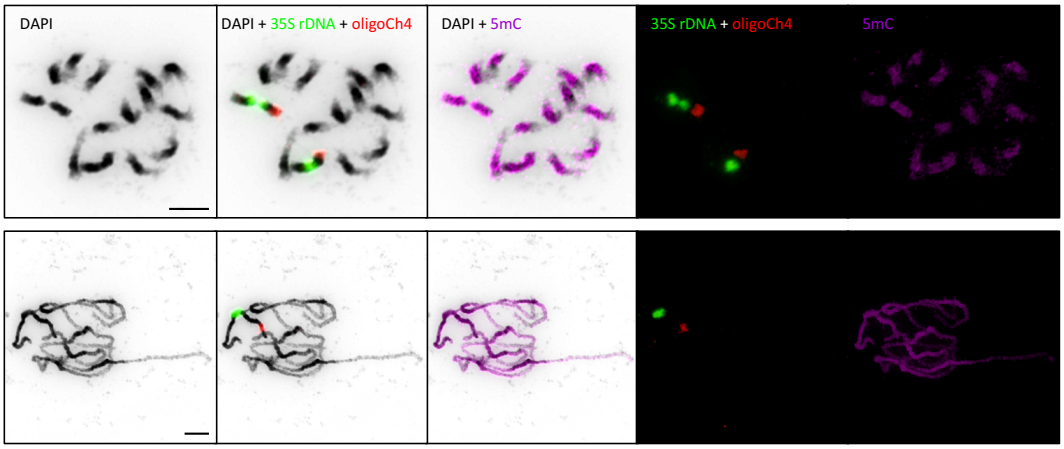

Aquilegia vulgaris

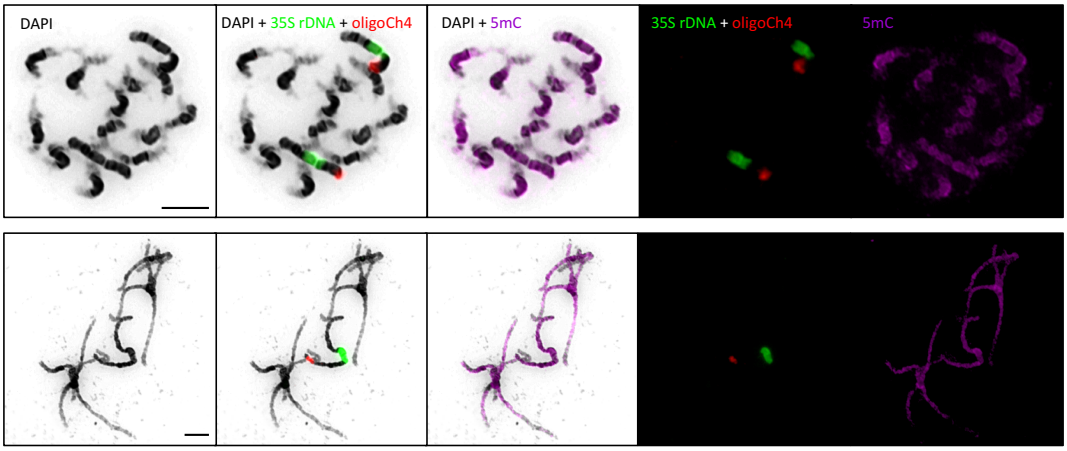

Aquilegia formosa